

Broadband Control of Group Delay Using the Brewster Effect in Metafilms

Yasuhiro Tamayama[✉]* and Hiromu Yamamoto

¹*Department of Electrical, Electronics and Information Engineering, Nagaoka University of Technology, 1603-1 Kamitomioka, Nagaoka, Niigata 940-2188, Japan*



(Received 25 January 2022; revised 8 April 2022; accepted 27 May 2022; published 13 July 2022)

We propose and verify a method for controlling the frequency dependence of the group delay of electromagnetic waves over a broad frequency range using the Brewster effect in single-layer metamaterials with finite thickness, here referred to as metafilms. When the reflectance of the metafilm vanishes regardless of the incident frequency, the group delay can be large near its resonance frequency while maintaining the transmittance close to unity regardless of the incident frequency. Furthermore, when several reflectionless metafilms are stacked together, the total group delay should be given as the sum of the individual group delays. In this study, we realize reflectionless metafilms by arranging the meta-atoms so that the Brewster effect occurs regardless of the incident frequency. We evaluate in numerical simulations and experiments the frequency dependence of the transmittance and of the group delay of a three-layer metamaterial composed of reflectionless metafilms with different resonance frequencies and find that the total transmittance and group delay of this metamaterial agree, respectively, with the product of the transmittances and the sum of the group delays of the constituent metafilms.

DOI: 10.1103/PhysRevApplied.18.014029

I. INTRODUCTION

The slow-group-velocity propagation [1] and storage [2,3] of electromagnetic waves have been realized using a quantum interference effect known as electromagnetically induced transparency (EIT) [4]. To date, extensive efforts have been devoted to mimicking EIT in metamaterials for the realization of slow-group-velocity propagation and other related phenomena over various frequency bands. These efforts have been based on mechanical and electrical circuit models of EIT [5]. To realize a metamaterial that mimics EIT, these classical models have revealed that the unit cell of the metamaterial should be composed of two resonators, one of low Q that is excited by incident waves, which is coupled to the other one, of high Q , that is not excited directly by the incident waves [6–13]. Metamaterials with an EIT-like transmission property have also been realized by arranging two coupled resonators to be excited directly by the incident waves [14–17]. Storage of the electromagnetic waves has even been realized using metamaterials that mimic EIT [18,19], as has been demonstrated using the original EIT effect.

Although EIT-like metamaterials play an important role in controlling the group velocity (the group delay) of electromagnetic waves, there are hints that they may not be the best solution. In EIT-like metamaterials, the large group delay occurs over a narrow frequency range and incident

electromagnetic waves outside of this narrow frequency range are reflected. Therefore, it may be difficult to control the frequency dependence of the group delay using EIT-like metamaterials over a broad frequency range.

Recently, metasurfaces with multiple Lorentzian electric and magnetic resonances have enabled the broadband control of group delay [20,21]. In this study, we demonstrate the broadband control of group delay using the Brewster effect in a single-layer metamaterial with only an electric response in order to simplify the design of the frequency dependence of the group delay. Hereafter, we refer to a single-layer metamaterial with finite thickness as a metafilm. So far, the Brewster effect has been investigated in various kinds of metamaterials and metasurfaces [22–29]. As a part of these studies, we have shown in our previous papers [30,31] that reflection in a metafilm can be completely suppressed by arranging the meta-atoms so that the oscillation direction of the electric dipole (or magnetic dipole) induced in the meta-atoms coincides with the propagation direction of the reflected wave. This idea is based on the physical mechanism underlying the Brewster effect. Hereafter, we refer to a metafilm that is designed to ensure that the Brewster effect occurs as a Brewster metafilm. When the oscillation direction of the electric dipole induced in the meta-atom is independent of the incident frequency, the reflectance of the metafilm vanishes regardless of the incident frequency. In this instance, the absolute value of the transmittance is unity regardless of the incident frequency and the group delay becomes large

*tamayama@vos.nagaokaut.ac.jp

near the resonance frequency of the Brewster metafilm if the nonradiation losses of the constituent meta-atoms are sufficiently small [31]. This implies that the broadband control of group delay can be achieved by stacking Brewster metafilms with different resonance frequencies. In the following, we verify this idea through numerical analyses and microwave experiments.

II. THEORY

First, we analyze the transmission property of a reflectionless metafilm using a model (Fig. 1) in which we assume that there exist a propagation mode and a resonance mode. The resonance mode corresponds to a resonant metafilm. To model the reflectionless property of the metafilm, the radiated wave from the resonator is assumed to propagate only in the direction of propagation of the transmitted wave. Based on the coupled-mode theory [32–34], we obtain the governing equations

$$\frac{da}{d\tau} = (-i\omega_0 - \gamma_r - \gamma_{nr})a + \kappa s_{1in}, \quad (1)$$

$$s_{1out} = 0, \quad (2)$$

$$s_{2out} = s_{1in} + \eta a, \quad (3)$$

where s_{1in} is the amplitude of the incident wave, s_{1out} is the amplitude of the reflected wave, s_{2out} is the amplitude of the transmitted wave, a is the amplitude of the resonance mode, ω_0 is the resonance angular frequency of the resonator, γ_r (γ_{nr}) is the radiation loss (nonradiation loss) of the resonator, κ (η) is the coupling between the incident (transmitted) wave and the resonance mode, and τ is time. Using the relation $\kappa\eta = -2\gamma_r$, which is derived from energy conservation and time-reversal symmetry, the amplitude transmittance for a continuous wave with angular frequency of ω is calculated to be

$$t = \frac{s_{2out}}{s_{1in}} = \frac{-i(\omega - \omega_0) - \gamma_r + \gamma_{nr}}{-i(\omega - \omega_0) + \gamma_r + \gamma_{nr}}. \quad (4)$$

Figures 2(a)–2(d) show the angular-frequency dependence of the complex transmittance given by Eq. (4) for various values of γ_{nr}/γ_r . The absolute value of the amplitude transmittance $|t|$ is unity regardless of the angular

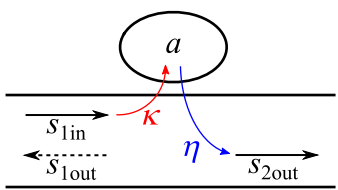


FIG. 1. A schematic of a resonator system coupled to two ports. To model the reflectionless property of the resonator, the radiated wave from the resonator is assumed to propagate only in the propagation direction of the transmitted wave.

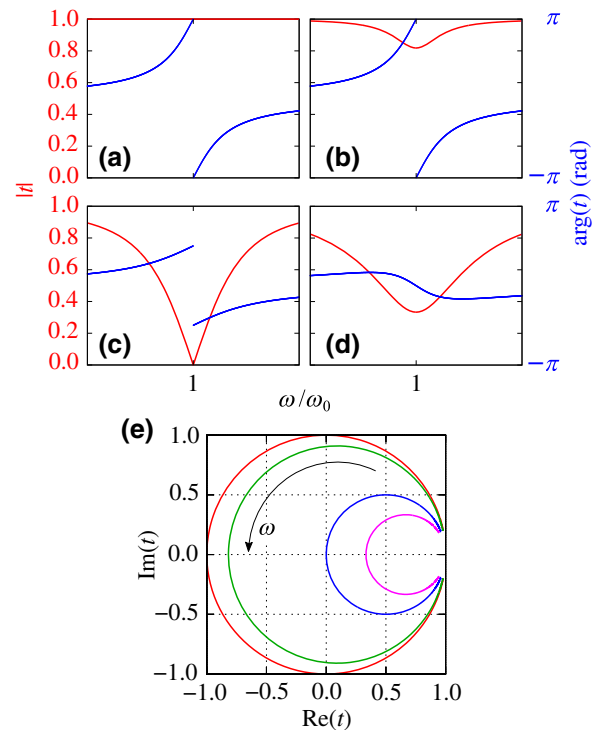


FIG. 2. (a)–(d) The angular-frequency dependence of the complex transmittance given by Eq. (4) for γ_{nr}/γ_r of (a) 0, (b) 0.1, (c) 1, and (d) 2. (e) The locus of the complex transmittance as a function of the angular frequency in the complex plane. The curves correspond to $\gamma_{nr}/\gamma_r = 0, 0.1, 1$, and 2 in order from large to small radius. The angular-frequency range in (a)–(d) is $\omega_0 - 4\gamma_r < \omega < \omega_0 + 4\gamma_r$ and that in (e) is $\omega_0 - 10\gamma_r < \omega < \omega_0 + 10\gamma_r$. $\omega_0/\gamma_r = 10$ is assumed in the calculation.

frequency for $\gamma_{nr}/\gamma_r = 0$ and $|t|$ at $\omega = \omega_0$ decreases with increasing γ_{nr}/γ_r for $\gamma_{nr}/\gamma_r < 1$. At $\omega = \omega_0$, $|t|$ vanishes; that is, perfect absorption occurs at $\omega = \omega_0$ for $\gamma_{nr}/\gamma_r = 1$, which is referred to as critical coupling [34]. For $\gamma_{nr}/\gamma_r > 1$, $|t|$ at $\omega = \omega_0$ increases with increasing γ_{nr}/γ_r . The group delay, which is given by $d[\arg(t)]/d\omega$, has a large positive value near $\omega = \omega_0$ for $\gamma_{nr}/\gamma_r < 1$ and becomes negative near $\omega = \omega_0$ for $\gamma_{nr}/\gamma_r > 1$.

The angular-frequency dependence of the complex transmittance is quite different depending on whether $\gamma_{nr}/\gamma_r < 1$ or $\gamma_{nr}/\gamma_r > 1$. The reason for this difference is understood from the locus of t in the complex plane [Fig. 2(e)]. The position of t moves in a counterclockwise direction in the complex plane as the angular frequency increases. The size of the locus of t decreases with increasing γ_{nr}/γ_r . This figure implies that the difference is caused by whether the point at the intersection of the locus of t with the real axis is positive or negative. (Note that the intersection corresponds to $\omega = \omega_0$.) The group delay near $\omega = \omega_0$ is found to be positive (negative) when the intersection is on the negative (positive) real axis because the point of t moves in a counterclockwise direction with

increasing angular frequency. The complex transmittance at $\omega = \omega_0$ is also found to vary only between -1 and 1 as γ_{nr}/γ_r increases.

From the above analysis, the transmittance and group delay of a metafilm near the resonance frequency are found to be controlled through varying γ_{nr}/γ_r if the reflection is completely suppressed regardless of the incident frequency. When such reflectionless metafilms are stacked, the total complex transmittance of the stacked metafilms should be given by the product of the complex transmittances of the constituent metafilms, because of the reflectionless property of the metafilms. This implies that a multilayer metamaterial with a specified complex transmission spectrum may be designed by controlling the ω_0 and γ_{nr}/γ_r values of each metafilm layer. In particular, for group-delay control over a broad frequency range, we only need to stack reflectionless metafilms with different resonance frequencies and $\gamma_{nr}/\gamma_r \ll 1$.

III. SIMULATION AND EXPERIMENT

From numerical and experimental work, we verify the above theory for broadband control of group delay using Brewster metafilms as reflectionless metafilms. We use meander-line resonators [Fig. 3(a)] as the meta-atoms that constitute the Brewster metafilms because such resonators have a relatively high radiation loss, which is advantageous in decreasing γ_{nr}/γ_r . When an x -polarized electromagnetic wave is incident on the meander-line resonator, an electric dipole is induced in the x direction. Therefore, a Brewster metafilm may be fabricated by arranging the meander-line resonators so that the propagation direction of the reflected wave coincides with the x direction [Fig. 3(b)]. To minimize γ_{nr}/γ_r for a given γ_{nr} , that is, to maximize γ_r , the propagation direction of both the incident and the transmitted waves should coincide with the direction for which the radiation pattern of the electric dipole induced in the resonator is maximal [35]. Therefore, in the following, we set $\theta = 45^\circ$.

Using the COMSOL Multiphysics commercial finite-element software, we analyze the reflection and transmission properties of the designed metafilms. In this numerical analysis, we assume that the meander-line resonator is made of a perfect electric conductor with vanishing thickness and that the substrate is FR-4, with a relative permittivity of $4.5(1 + i0.03)$.

We calculate the copolarized amplitude reflectance r_{co} , the copolarized amplitude transmittance t_{co} , and the cross-polarized amplitude transmittance t_{cross} of a plane wave incident on metafilms with $w_m = 3.0$ mm, 2.5 mm, and 2.0 mm (Fig. 4). For all instances, $|r_{co}|$ and $|t_{cross}|$ in the calculated frequency range are less than about 0.1 , which implies that the reflection and the polarization conversion is small. From this result, Brewster metafilms may be fabricated using meander-line resonators as meta-atoms. The

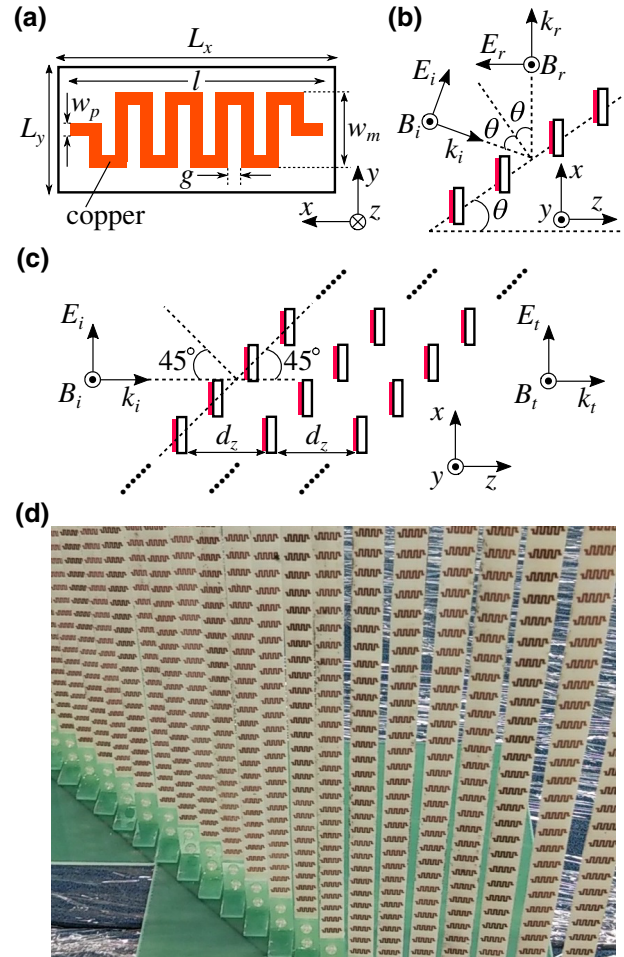


FIG. 3. (a) A schematic of the structure of the meta-atom used in studying the broadband control of group delay. The parameter settings used are as follows: $w_p = 0.5$ mm, $g = 0.5$ mm, $l = 9.5$ mm, $L_x = 11.5$ mm, and $L_y = 7.5$ mm. The range of values for w_m is given in the main text. The thickness of the substrate is 0.8 mm. (b) The relationship between the electromagnetic fields and the distribution of the meta-atoms needed to produce the Brewster effect in a metafilm. (c) A schematic of the three-layer metamaterial composed of three Brewster metafilms. The subscripts “ i ”, “ r ”, and “ t ” indicate the incident, reflected, and transmitted fields, respectively. (d) A photograph of one of the fabricated Brewster metafilms.

group delay, which is given by $d[\arg(t_{co})]/d\omega$, peaks at resonance frequencies 7.10 GHz, 7.90 GHz, and 8.74 GHz when $w_m = 3.0$ mm, 2.5 mm, and 2.0 mm, respectively. [Throughout, the value of the group delay is defined as the difference between the group delays from the transmitter to the receiver of the system with and without the metafilm(s).] The value of $|t_{co}|$ at resonance decreases from unity because of the dielectric loss of the substrate (to be discussed later).

Next, we analyze the transmission properties of a three-layer metamaterial composed of all three metafilms set with $w_m = 3.0$ mm, 2.5 mm, and 2.0 mm. As shown in

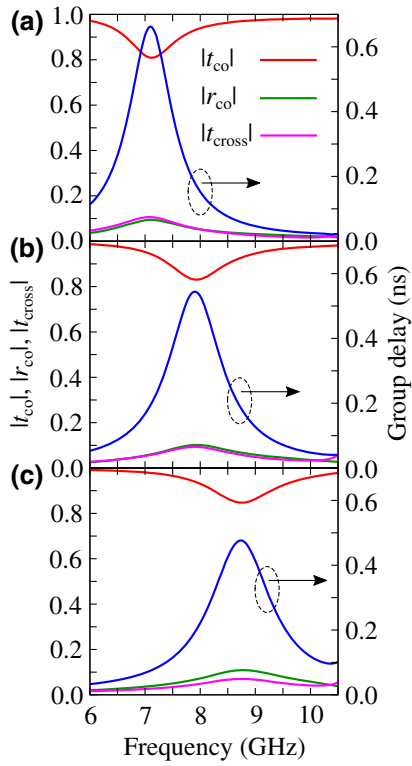


FIG. 4. The transmission and reflection spectra of Brewster metafilms obtained from numerical calculations with w_m of (a) 3.0 mm, (b) 2.5 mm, and (c) 2.0 mm. The relative permittivity of the substrate is assumed to be $4.5(1 + i0.03)$ for this calculation.

Fig. 3(c), the metafilms are assumed to be placed with the interlayer distance between adjacent metafilms in the z direction of d_z . Because of the reflectionless property of the metafilms, $|t_{co}|$ and the group delay of the three-layer metamaterial should agree with the product of the individual transmittances $|t_{co}|$ and the sum of the individual group delays of the constituent metafilms, respectively. Figure 5 shows plots of the transmittance $|t_{co}|$ and the group delay for the three-layer metamaterial with $d_z = 10$ mm, 20 mm, and 40 mm obtained from numerical calculations. For $d_z = 10$ mm, the difference between the transmittance $|t_{co}|$ (the group delay) of the three-layer metamaterial and the product of transmittances $|t_{co}|$ (the sum of the group delays) of the constituent metafilms is large. The difference becomes quite small when d_z exceeds 20 mm, which is smaller than the wavelength at 8 GHz (37.5 mm). For $d_z = 40$ mm, the transmittance $|t_{co}|$ (the group delay) of the three-layer metamaterial almost agrees with the product of transmittances $|t_{co}|$ (the sum of the group delays) of the constituent metafilms. This result implies that the difference arises from the interlayer coupling between the constituent metafilms. Therefore, when the constituent metafilms are not mutually coupled, the transmittance (the group delay) of a multilayer metamaterial composed of stacked Brewster metafilms may agree

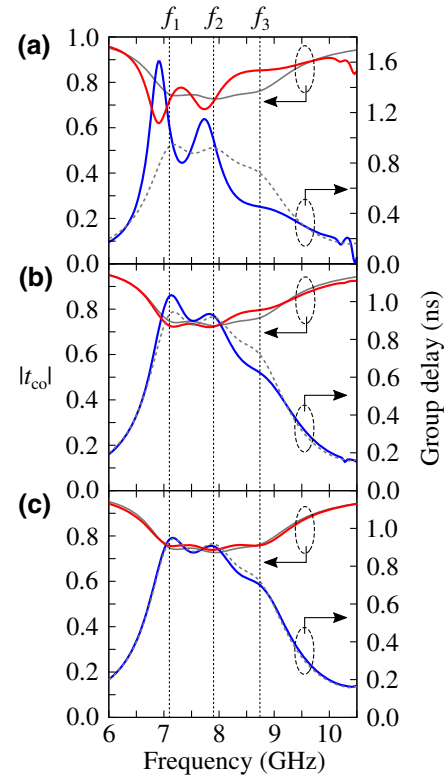


FIG. 5. The transmission spectra of the three-layer metamaterial obtained from numerical calculations with (a) $d_z = 10$ mm, (b) 20 mm, and (c) 40 mm. The gray solid and dashed curves are the respective plots of the product of the individual transmittances $|t_{co}|$ and the sum of the individual group delays of the three constituent Brewster metafilms. The resonance frequencies of the Brewster metafilms with $w_m = 3.0$ mm, 2.5 mm, and 2.0 mm are $f_1 = 7.10$ GHz, $f_2 = 7.90$ GHz, and $f_3 = 8.74$ GHz, respectively. The relative permittivity of the substrate is assumed to be $4.5(1 + i0.03)$ for this calculation.

with the product of the transmittances (the sum of the group delays) of the constituent metafilms.

Following the numerical verification of the theory, we fabricate the designed metafilms to verify the theory through experiments. The meta-atoms are fabricated using printed circuit boards that consist of a 35- μm -thick copper film on a 0.8-mm-thick FR-4 substrate. A photograph of one of the fabricated metafilms is shown in Fig. 3(d). Although the meta-atoms are fixed to the stage in this study to simplify our proof-of-principle experiment, in practical applications, the meta-atoms may be fixed to a frame.

Figures 6(a)–6(c) show the measured frequency dependencies of $|t_{co}|$ and the group delay for the three metafilms, individually with $w_m = 3.0$ mm, 2.5 mm, and 2.0 mm; their respective group delays peak at resonance frequencies of 7.4 GHz, 8.4 GHz, and 9.1 GHz. The transmittances at these resonance frequencies decrease from unity through dielectric losses in the substrate, as observed from the numerical simulation. The measured and simulation results almost agree, implying that Brewster metafilms

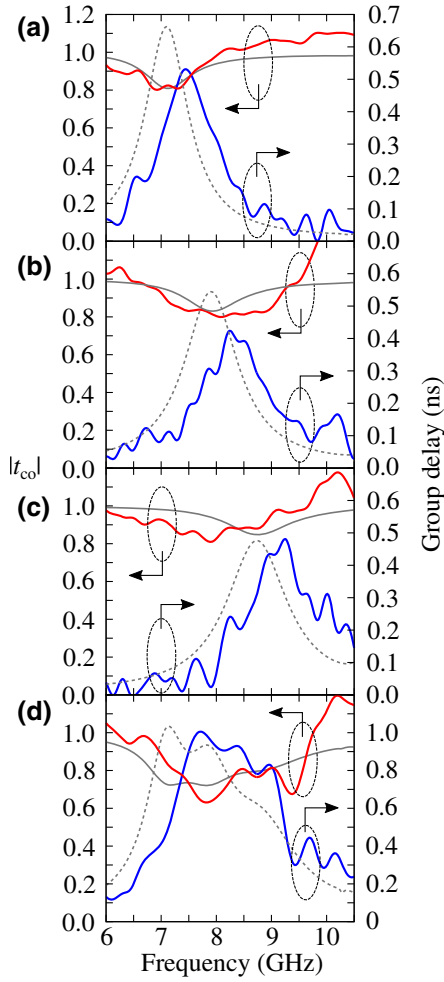


FIG. 6. The measured frequency dependencies of transmittance $|t_{co}|$ and the group delay of the Brewster metafilms, individually with (a) $w_m = 3.0$ mm, (b) 2.5 mm, and (c) 2.0 mm, and (d) those for the three-layer metamaterial with $d_z = 20$ mm. The value of $|t_{co}|$ is defined as the ratio of the transmittances with and without the metafilm(s) between the transmitting and receiving antennas. Because the size of the metafilm(s) and the beam width of the electromagnetic wave are finite, $|t_{co}|$ exceeds unity in some frequency regions. The gray solid and dashed curves are plots of $|t_{co}|$ and the group delay presented in Figs. 4 and 5(b) for reference.

have been realized in these experiments using meander-line resonators as meta-atoms.

We then measure the transmission properties of a three-layer metamaterial composed of the three metafilms with $w_m = 3.0$ mm, 2.5 mm, and 2.0 mm. In the results of the numerical simulation, the transmittance (the group delay) of the three-layer metamaterial almost agrees with the product of the individual transmittances (the sum of the individual group delays) of the constituent metafilms when the interlayer distance d_z is larger than 20 mm. Therefore, in the experiment, d_z is set to 20 mm. The measured frequency dependencies of the transmittance and group

delay of the three-layer metamaterial [Fig. 6(d)] show that the transmittance does not exhibit a steep variation and that the group delay becomes large in value over a broader frequency range than in instances using a single metafilm, because of the difference in the resonance frequencies of the constituent metafilms. Also, the measured transmittance and group delay roughly agree with the numerical results. This theory for broadband control of group delay using multilayer Brewster metafilms is thus verified in both numerical simulations and experiments.

In fabricating the Brewster metafilms for this study, we use printed circuit boards with a FR-4 substrate because they are widely available at low cost. Although they are satisfactory for our proof-of-principle experiment, we note that the transmittances of the designed Brewster metafilms decrease from unity near the resonance frequency because of nonradiation losses in the metafilms. According to the above theory, the transmittance at the resonance frequency increases with decreasing γ_{nr}/γ_r for $\gamma_{nr}/\gamma_r < 1$. To estimate the attainable transmittance at the resonance frequency under realistic conditions, we analyze numerically the electromagnetic responses of the Brewster metafilms made of commercially available low-loss laminates; specifically, Rogers RT/duroid 5880. For the analysis, the relative permittivity of the substrate of the laminate is assumed to be $2.2(1 + i0.0009)$.

Figure 7(a) shows the numerically calculated transmission and reflection properties of the metafilm with $w_m = 3.0$ mm. Both $|r_{co}|$ and $|t_{cross}|$ are low in value in the calculated frequency range, as for the FR-4 substrate; moreover, $|t_{co}|$ at the resonance frequency (8.13 GHz) is higher than 0.98 , which is higher than for the FR-4 substrate. From this result, the decrease in $|t_{co}|$ at the resonance frequency for the printed circuit board with the FR-4 substrate is found to occur because of dielectric losses in the substrate and, for the commercially available printed circuit board with the low-loss substrate, $|t_{co}|$ is found to be near unity at the resonance frequency. Figure 7(b) shows the transmission property of a three-layer metamaterial composed of metafilms with $w_m = 3.0$ mm, 2.5 mm, and 2.0 mm. Because of lower dielectric losses in the substrate, the group delay becomes large over a broad frequency range while $|t_{co}|$ remains closer to unity than for the FR-4 substrate. The transmittance (the group delay) of the three-layer metamaterial also agrees in this instance with the product of the transmittances (the sum of the group delays) of the constituent metafilms.

IV. DISCUSSION

We discuss the results of this study and of previous studies using the delay-bandwidth product as an index of the broadband control of group delay. A delay-bandwidth product of 0.45 (the maximum group delay is 0.333 ns and the full width at half maximum of the transmittance

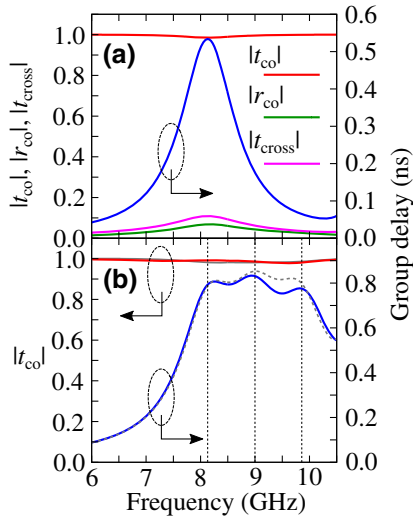


FIG. 7. (a) The transmission and reflection spectra of the Brewster metafilms with $w_m = 3.0$ mm. (b) The transmission spectrum of the three-layer metamaterial with $d_z = 40$ mm obtained from numerical calculations. The gray solid and dashed curves are the product of the transmittances $|t_{col}|$ and the sum of the group delays of the Brewster metafilms with $w_m = 3.0$ mm, 2.5 mm, and 2.0 mm, respectively. The vertical dashed lines indicate the respective resonance frequencies, 8.13 GHz, 9.00 GHz, and 9.86 GHz, of these Brewster metafilms. The relative permittivity of the substrate is assumed to be $2.2(1 + i0.0009)$ for this calculation.

is 1.35 GHz) has been achieved in a single-layer EIT-like metasurface [12]. As described in Ref. [20], the variation range of the transmission phase in metasurfaces with only an electric response is limited to π . This implies that the transmission bandwidth decreases with an increase of the maximum group delay in EIT-like metasurfaces. Therefore, the delay-bandwidth product cannot be increased significantly as long as single-layer EIT-like metasurfaces are used. In addition, the delay-bandwidth product cannot be increased by increasing the number of layers of EIT-like metasurfaces, because the reflectance vanishes only at the transmission peak frequency and the multiple reflection occurs at the other frequencies. In contrast, the result in this study implies that the delay-bandwidth product can be increased arbitrarily by increasing the number of metafilm layers.

Previously, a theory for realizing arbitrarily large delay-bandwidth product using metasurfaces has also been proposed and verified [20,21]. We now look into the performance of the group-delay control presented in this study and in Refs. [20,21]. The metasurfaces used in Refs. [20,21] are composed of planar structures with Lorentzian electric and magnetic resonances. Transmission-type and reflection-type metasurfaces for the group-delay control are theoretically designed and the reflection-type metasurface is experimentally verified. The

maximum group delay, the full width at half maximum of the group delay, and the delay-bandwidth product of the reflection-type metasurface are 2.0 ns, 700 MHz, and 1.4, respectively. The metamaterial used in this study is of transmission type, with a nonplanar structure, and is composed of resonators with only an electric response. The maximum group delay, the full width at half maximum of the group delay, and the delay-bandwidth product of the three-layer metamaterial are 1.0 ns, 2.1 GHz, and 2.1, respectively [Fig. 6(d)]. In contrast to Ref. [12], the frequency bandwidth is determined from the frequency dependence of the group delay because the transmittance in this study (the reflectance in Ref. [21]) does not vary so much as the frequency varies. The delay-bandwidth products achieved in this study and Ref. [21] are the same within a factor of 2 and larger than for the single-layer EIT-like metasurface in Ref. [12].

Note that the delay-bandwidth product can be further increased by increasing the number of metafilm layers in this study (by increasing the number of resonators in the unit cell in Ref. [21]). The frequency bandwidth can be arbitrarily increased in both theories in principle; however, the diffraction and the higher-order resonances may limit the frequency bandwidth in practical situations.

In short, the performance of the group-delay control using the metamaterial in this study and using the metasurfaces in Refs. [20,21] are comparable. Although the fabrication of the metamaterial in this study is more difficult than for the metasurfaces in Refs. [20,21], the metamaterial in this study can be composed of meta-atoms with only an electric response. Therefore, the metamaterial in this study would enable us to design the complicated frequency dependence of group delay more easily.

V. CONCLUSIONS

From numerical simulations and experiments, we verify a theory concerning the control of group delay over a broad frequency range using Brewster metafilms. The transmittance of the Brewster metafilm with $\gamma_{nr}/\gamma_r \ll 1$ is almost unity regardless of the frequency and its group delay becomes large near the resonance frequency. Therefore, by stacking Brewster metafilms having different resonance frequencies, the frequency dependence of the group delay may be controlled over a broad frequency range while maintaining the transmittance close to unity. To verify this theory, we investigate a three-layer metamaterial composed of three Brewster metafilms with different resonance frequencies. When the near-field coupling between the constituent metafilms is sufficiently weak, the transmittance and the group delay of the three-layer metamaterial agree with the product of the transmittances and the sum of the group delays of the constituent metafilms, respectively.

We demonstrate that the frequency bandwidth for large group delay can be broadened by stacking Brewster

metafilms as a proof-of-principle experiment of the broadband control of group delay. Furthermore, this theory also applies to other kinds of control of the group delay. For example, a multilayer metamaterial with positive (negative) group-delay dispersion may be realized by stacking Brewster metafilms with different resonance frequencies so that the group delay in the higher-frequency range becomes larger (smaller). Also, when we divide a dispersionless metamaterial composed of multiple Brewster metafilms into two metamaterials and place one behind the transmitter and the other in front of the receiver, the envelope of the electromagnetic wave generated from the transmitter is distorted intentionally in the region between the two metamaterials but this distortion is compensated at the receiver, in a manner reminiscent of an analog encryption-decryption system.

As described in our previous paper [31], the macroscopic properties of Brewster metafilms are similar to those of Huygens metasurfaces with spectrally overlapping electric and magnetic resonances [36–43]. In designing Huygens metasurfaces, both the electric and magnetic responses in the metasurfaces need to be controlled. In contrast, Brewster metafilms can be designed based on either their electric or magnetic responses and may be useful in realizing anisotropic reflectionless metamaterials. This implies that the degree of freedom of polarization may be easily added to broadband control of electromagnetic waves. Although the fabrication of Brewster metafilms is more difficult than for Huygens metasurfaces, it is possible to fabricate terahertz (optical) Brewster metafilms using microelectromechanical systems [44] (3D laser lithography [45] and 3D nanoprinting techniques [46]). There are many studies on the control of electromagnetic waves using Huygens metasurfaces [47], which shows the importance of reflectionless metamaterials in controlling electromagnetic waves. Investigations of Brewster metafilms as well as Huygens metasurfaces would yield further advances in the control of electromagnetic waves.

ACKNOWLEDGMENTS

This research was supported by the Grant for Basic Science Research Projects from The Sumitomo Foundation, and the Japan Society for the Promotion of Science (JSPS) Grants-in-Aid for Scientific Research (KAKENHI) under Grants No. JP18H03690 and No. JP21K04192, and by the Japan Science and Technology Agency (CREST Grant No. JPMJCR2101).

[1] L. V. Hau, S. E. Harris, Z. Dutton, and C. H. Behroozi, Light speed reduction to 17 m per second in an ultracold atomic gas, *Nature* **397**, 594 (1999).

- [2] C. Liu, Z. Dutton, C. H. Behroozi, and L. V. Hau, Observation of coherent optical information storage in an atomic medium using halted light pulses, *Nature* **409**, 490 (2001).
- [3] D. F. Phillips, A. Fleischhauer, A. Mair, R. L. Walsworth, and M. D. Lukin, Storage of Light in Atomic Vapor, *Phys. Rev. Lett.* **86**, 783 (2001).
- [4] M. Fleischhauer, A. Imamoglu, and J. P. Marangos, Electromagnetically induced transparency: Optics in coherent media, *Rev. Mod. Phys.* **77**, 633 (2005).
- [5] C. L. Garrido Alzar, M. A. G. Martinez, and P. Nussenzveig, Classical analog of electromagnetically induced transparency, *Am. J. Phys.* **70**, 37 (2002).
- [6] S. Zhang, D. A. Genov, Y. Wang, M. Liu, and X. Zhang, Plasmon-Induced Transparency in Metamaterials, *Phys. Rev. Lett.* **101**, 047401 (2008).
- [7] P. Tassin, L. Zhang, T. Koschny, E. N. Economou, and C. M. Soukoulis, Low-Loss Metamaterials Based on Classical Electromagnetically Induced Transparency, *Phys. Rev. Lett.* **102**, 053901 (2009).
- [8] N. Liu, L. Langguth, T. Weiss, J. Kästel, M. Fleischhauer, T. Pfau, and H. Giessen, Plasmonic analogue of electromagnetically induced transparency at the Drude damping limit, *Nat. Mater.* **8**, 758 (2009).
- [9] Y. Lu, J. Y. Rhee, W. H. Jang, and Y. P. Lee, Active manipulation of plasmonic electromagnetically-induced transparency based on magnetic plasmon resonance, *Opt. Express* **18**, 20912 (2010).
- [10] Y. Tamayama, T. Nakanishi, and M. Kitano, Variable group delay in a metamaterial with field-gradient-induced transparency, *Phys. Rev. B* **85**, 073102 (2012).
- [11] G. Rana, P. Deshmukh, S. Palkhivala, A. Gupta, S. P. Duttagupta, S. S. Prabhu, V. G. Achanta, and G. S. Agarwal, Quadrupole-Quadrupole Interactions to Control Plasmon-Induced Transparency, *Phys. Rev. Appl.* **9**, 064015 (2018).
- [12] F. Bagci and B. Akaoglu, A polarization independent electromagnetically induced transparency-like metamaterial with large group delay and delay-bandwidth product, *J. Appl. Phys.* **123**, 173101 (2018).
- [13] Z. Xu, S. Liu, S. Li, and X. Yin, Analog of electromagnetically induced transparency based on magnetic plasmonic artificial molecules with symmetric and antisymmetric states, *Phys. Rev. B* **99**, 041104(R) (2019).
- [14] X.-R. Jin, Y. Lu, J. Park, H. Zheng, F. Gao, Y. Lee, J. Y. Rhee, K. W. Kim, H. Cheong, and W. H. Jang, Manipulation of electromagnetically-induced transparency in planar metamaterials based on phase coupling, *J. Appl. Phys.* **111**, 073101 (2012).
- [15] Y. Tamayama, K. Yasui, T. Nakanishi, and M. Kitano, Electromagnetically induced transparency like transmission in a metamaterial composed of cut-wire pairs with indirect coupling, *Phys. Rev. B* **89**, 075120 (2014).
- [16] Y. Tamayama, K. Hamada, and K. Yasui, Suppression of narrow-band transparency in a metasurface induced by a strongly enhanced electric field, *Phys. Rev. B* **92**, 125124 (2015).
- [17] M. Parvinnezhad Hokmabadi, E. Philip, E. Rivera, P. Kung, and S. M. Kim, Plasmon-induced transparency by hybridizing concentric-twisted double split ring resonators, *Sci. Rep.* **5**, 15735 (2015).
- [18] T. Nakanishi, T. Otani, Y. Tamayama, and M. Kitano, Storage of electromagnetic waves in a metamaterial that mimics

- electromagnetically induced transparency, *Phys. Rev. B* **87**, 161110(R) (2013).
- [19] T. Nakanishi and M. Kitano, Storage and retrieval of electromagnetic waves using electromagnetically induced transparency in a nonlinear metamaterial, *Appl. Phys. Lett.* **112**, 201905 (2018).
- [20] V. Ginis, P. Tassin, T. Koschny, and C. M. Soukoulis, Broadband metasurfaces enabling arbitrarily large delay-bandwidth products, *Appl. Phys. Lett.* **108**, 031601 (2016).
- [21] O. Tsilipakos, L. Zhang, M. Kafesaki, C. M. Soukoulis, and T. Koschny, Experimental implementation of achromatic multiresonant metasurface for broadband pulse delay, *ACS Photonics* **8**, 1649 (2021).
- [22] Y. Tamayama, T. Nakanishi, K. Sugiyama, and M. Kitano, Observation of Brewster's effect for transverse-electric electromagnetic waves in metamaterials: Experiment and theory, *Phys. Rev. B* **73**, 193104 (2006).
- [23] A. Alù, G. D'Aguanno, N. Mattiucci, and M. J. Bloemberger, Plasmonic Brewster Angle: Broadband Extraordinary Transmission through Optical Gratings, *Phys. Rev. Lett.* **106**, 123902 (2011).
- [24] R. Paniagua-Domínguez, Y. F. Yu, A. E. Miroshnichenko, L. A. Krivitsky, Y. H. Fu, V. Valuckas, L. Gonzaga, Y. T. Toh, A. Y. S. Kay, B. Luk'yanchuk, and A. I. Kuznetsov, Generalized Brewster effect in dielectric metasurfaces, *Nat. Commun.* **7**, 10362 (2016).
- [25] C. Wang, Z. Zhu, W. Cui, Y. Yang, L. Ran, and D. Ye, All-angle Brewster effect observed on a terahertz metasurface, *Appl. Phys. Lett.* **114**, 191902 (2019).
- [26] S. Yin and J. Qi, Metagrating-enabled Brewster's angle for arbitrary polarized electromagnetic waves and its manipulation, *Opt. Express* **27**, 18113 (2019).
- [27] G. Lavigne and C. Caloz, Generalized Brewster effect using bianisotropic metasurfaces, *Opt. Express* **29**, 11361 (2021).
- [28] H. Fan, J. Li, Y. Lai, and J. Luo, Optical Brewster Metasurfaces Exhibiting Ultrabroadband Reflectionless Absorption and Extreme Angular Asymmetry, *Phys. Rev. Appl.* **16**, 044064 (2021).
- [29] Z. Zhang, Z. Che, X. Liang, J. Chu, J. Zeng, H. Huang, F. Guan, L. Shi, X. Liu, and J. Zi, Realizing Generalized Brewster Effect by Generalized Kerker Effect, *Phys. Rev. Appl.* **16**, 054017 (2021).
- [30] Y. Tamayama, Brewster effect in metafilms composed of bianisotropic split-ring resonators, *Opt. Lett.* **40**, 1382 (2015).
- [31] Y. Tamayama, Design and analysis of frequency-independent reflectionless single-layer metafilms, *Opt. Lett.* **41**, 1102 (2016).
- [32] W. Suh, Z. Wang, and S. Fan, Temporal coupled-mode theory and the presence of non-orthogonal modes in lossless multimode cavities, *IEEE J. Quantum Electron.* **40**, 1511 (2004).
- [33] Z. Ruan and S. Fan, Temporal coupled-mode theory for Fano resonance in light scattering by a single obstacle, *J. Phys. Chem. C* **114**, 7324 (2010).
- [34] Z. Ruan and S. Fan, Superscattering of Light from Subwavelength Nanostructures, *Phys. Rev. Lett.* **105**, 013901 (2010).
- [35] Y. Tamayama and Y. Kida, Tunable group delay in a doubly resonant metasurface composed of two dissimilar split-ring resonators, *J. Opt. Soc. Am. B* **36**, 2694 (2019).
- [36] M. Decker, I. Staude, M. Falkner, J. Dominguez, D. N. Neshev, I. Brener, T. Pertsch, and Y. S. Kivshar, High-efficiency dielectric Huygens' surfaces, *Adv. Opt. Mater.* **3**, 813 (2015).
- [37] K. E. Chong, I. Staude, A. James, J. Dominguez, S. Liu, S. Campione, G. S. Subramania, T. S. Luk, M. Decker, D. N. Neshev, I. Brener, and Y. S. Kivshar, Polarization-independent silicon metadevices for efficient optical wavefront control, *Nano Lett.* **15**, 5369 (2015).
- [38] V. S. Asadchy, I. A. Faniaye, Y. Ra'di, S. A. Khakhomov, I. V. Semchenko, and S. A. Tretyakov, Broadband reflectionless metasheets: Frequency-selective transmission and perfect absorption, *Phys. Rev. X* **5**, 031005 (2015).
- [39] A. Balmakou, M. Podalov, S. Khakhomov, D. Stavenga, and I. Semchenko, Ground-plane-less bidirectional terahertz absorber based on omega resonators, *Opt. Lett.* **40**, 2084 (2015).
- [40] F. S. Cuesta, I. A. Faniaye, V. S. Asadchy, and S. A. Tretyakov, Planar broadband Huygens' metasurfaces for wave manipulations, *IEEE Trans. Antennas Propag.* **66**, 7117 (2018).
- [41] M. Londoño, A. Sayanskiy, J. L. Araque-Quijano, S. B. Glybovski, and J. D. Baena, Broadband Huygens' Metasurface Based on Hybrid Resonances, *Phys. Rev. Appl.* **10**, 034026 (2018).
- [42] A. A. Fathnan, M. Liu, and D. A. Powell, Achromatic Huygens' metalenses with deeply subwavelength thickness, *Adv. Opt. Mater.* **8**, 2000754 (2020).
- [43] J. P. del Risco, I. S. Mikhalka, V. A. Lenets, M. S. Sidorenko, A. D. Sayanskiy, S. B. Glybovski, A. L. Samoilov, S. A. Khakhomov, I. V. Semchenko, J. D. Ortiz, and J. D. Baena, Optimal angular stability of reflectionless metasurface absorbers, *Phys. Rev. B* **103**, 115426 (2021).
- [44] H. Tao, A. C. Strikwerda, K. Fan, W. J. Padilla, X. Zhang, and R. D. Averitt, Reconfigurable Terahertz Metamaterials, *Phys. Rev. Lett.* **103**, 147401 (2009).
- [45] J. K. Gansel, M. Thiel, M. S. Rill, M. Decker, K. Bade, V. Saile, G. von Freymann, S. Linden, and M. Wegener, Gold helix photonic metamaterial as broadband circular polarizer, *Science* **325**, 1513 (2009).
- [46] W. Jung, Y.-H. Jung, P. V. Pikhitsa, J. Feng, Y. Yang, M. Kim, H.-Y. Tsai, T. Tanaka, J. Shin, K.-Y. Kim, H. Choi, J. Rho, and M. Choi, Three-dimensional nanoprinting via charged aerosol jets, *Nature* **592**, 54 (2021).
- [47] M. Chen, M. Kim, A. M. H. Wong, and G. V. Eleftheriades, Huygens' metasurfaces from microwaves to optics: A review, *Nanophotonics* **7**, 1207 (2018).